ARTICLE

OBC
www.rsc.org/obc

Why a hexabromodiquinoline host preferentially includes small aromatic hydrocarbon guests

A. Noman M. M. Rahman, Roger Bishop,* Donald C. Craig and Marcia L. Scudder
School of Chemical Sciences, The University of New South Wales, UNSW Sydney NSW 2052, Australia. E-mail: r.bishop@unsw.edu.au

Received 10th January 2003, Accepted 6th March 2003
First published as an Advance Article on the web 26th March 2003

The preparation and properties of the new hexabromodiquinoline derivative **4** are described. This lattice inclusion host shows a strong preference for trapping small aromatic hydrocarbons. The X-ray crystal structures of the benzene, toluene, *o*-xylene, and *p*-xylene compounds are reported, and are analysed from a crystal engineering perspective. Crystallisation of **4** from the dual-nature solvent trifluoromethylbenzene yields the solvent-free material. Comparison of the parent crystal structure with those of its inclusion compounds reveals why inclusion of aromatic hydrocarbon guests is such a favoured process. The high concentration of Br ··· Br interactions in the structure of pure **4** is diluted and increasingly replaced by aromatic offset face–face (OFF) and aromatic edge–face (EF) interactions in the inclusion compounds, and this results in better lattice packing energies. For toluene, *o*-xylene, and *p*-xylene the host–guest ratio is 1 : 1. Inclusion of the smaller benzene molecule results in a change to 2 : 3 stoichiometry. This increase in guest content is assisted by replacement of host–host OFF and EF motifs with host–host pi-halogen dimer (PHD) interactions, which provide space for inclusion of the additional guest molecules. These changes result in the most efficient lattice packing of the series for compound $(\mathbf{4})_2\cdot(\text{benzene})_3$.

Introduction

Many inclusion compounds result from interaction of a guest with a pre-formed receptor structure belonging to the host molecule.[1,2] Familiar examples of such hosts are the crown ethers, cyclodextrins, calixarenes, and their many analogues. Host–guest systems of this general type are simple to understand or model, and can be fine-tuned comparatively easily to trap specific guest species. In contrast, lattice inclusion (clathrate) compounds are materials whose stability arises from the many host–guest interactions constituting their overall crystal lattice. This characteristic makes the design of new lattice inclusion hosts, and also their anticipated properties, rather more difficult to predict.[3,4]

Recently we have been investigating the chemistry of several families of C_2-symmetric diquinoline compounds.[5–7] In general, the parent systems (for example **1**) do not include guests, but their halogenated derivatives (for example **2**,**3**) are excellent lattice inclusion hosts.

These compounds were designed to rule out the involvement of strong hydrogen bonding, and thereby permit the investigation of other weaker intermolecular attractions, in their host–guest compounds. In these structures aryl offset face–face (OFF),[8,9] aryl edge–face (EF),[8,9] edge–edge C–H ··· N dimer,[5,6] pi–halogen dimer (PHD),[10] halogen–halogen,[11,12] pi–halogen,[13] and other weak interactions, compete with each other to produce the lattice inclusion structure of lowest energy.

In designing these new halogenated diquinoline hosts, we have increased the likelihood of molecular inclusion taking place. At the same time, however, we have reduced prediction of exactly how this will be achieved. In practice, we have encountered three types of outcome. Some hosts form the same general type of structure no matter what guest molecules are included. For example, two molecules of **2** always wrap around a guest molecule to enclose it in a penannular manner.[14,15] In contrast other hosts, such as **3**, include a wide range of guests by adopting a variety of different inclusion structures.[10,16]

The third event, and arguably the most novel, is where the host molecule shows a strong selectivity for guests of only one functional group type. This is the case for the hexabromo compound **4**, the subject of the present paper, which prefers to include small aromatic hydrocarbons.

Results and discussion

Preparation of the diquinoline host 4

The preparations of the diquinoline host molecules **2**–**4** are outlined in Scheme 1. Tetrabromo derivative **3**[10] was prepared by bromination of the racemic parent diquinoline **1**[15] using a mixture of bromine, silver sulfate, and 98% sulfuric acid. This protocol was originally devised by de la Mare *et al.*,[17,18] who used it to brominate quinoline cleanly at its 5- and 8- positions. Recently we have found that their method works equally well on diquinoline substrates.[19]

Reaction of **3** with *N*-bromosuccinimide (NBS) afforded the new hexabromo product **4** in 85% yield. In common with earlier NBS brominations of similar systems,[5] this radical reaction proceeded with both high regio- and stereo-specificity in forming the required product.

We have remarked earlier[19] that increasing the number of bromine atoms beyond four in these diquinoline systems is detrimental to molecular inclusion and, indeed, the hexabromide **4** rejected the majority of potential guests that it was offered. However, it did show some host properties and was found to have a very strong preference for trapping small aromatic hydrocarbon guests. Crystalline inclusion compounds of **4** with benzene, toluene, *o*-xylene, and *p*-xylene were obtained and their single crystal X-ray structures determined. Numerical details of the solution and refinement of these structures, plus that of solvent-free **4**, are presented in Table 1.

The following liquids were also tested for inclusion, but in no case was crystalline material obtained: dichloromethane, carbon tetrachloride, chloroform, 1,1,1-trichloroethane, 1,2-dichlorofluoroethane, 1,1,2,2-tetrachloroethane, tetrachloroethene, chlorobenzene, diiodomethane, dimethyl carbonate, methanol, ethanol, acetonitrile, acetone, ethyl acetate, dimethyl sulfoxide, dimethyl formamide, mesitylene, thiophene, tetrahydrofuran, dioxane, 1-butanol, 1,2-dimethoxyethane, pyridine, and methyl acrylate. Poor quality inclusion crystals were obtained from allyl cyanide solution.[20]

DOI: 10.1039/b300248a

Table 1 Numerical details of the solution and refinement of the crystal structures

Properties/compound	**4**	(**4**)·(C_8H_{10}) (*o*-xylene)	(**4**)·(C_8H_{10}) (*p*-xylene)	(**4**)·(C_7H_8)	(**4**)$_2$·(C_6H_6)$_3$
Molecular formula	$C_{22}H_{10}Br_6N_2$	$C_{22}H_{10}Br_6N_2$·(C_8H_{10})	$C_{22}H_{10}Br_6N_2$·(C_8H_{10})	$C_{22}H_{10}Br_6N_2$·(C_7H_8)	2($C_{22}H_{10}Br_6N_2$)·3(C_6H_6)
Asymmetric formula	$C_{22}H_{10}Br_6N_2$	$C_{22}H_{10}Br_6N_2$·(C_8H_{10})	$C_{22}H_{10}Br_6N_2$·(C_8H_{10})	$C_{22}H_{10}Br_6N_2$·(C_7H_8)	$C_{22}H_{10}Br_6N_2$·1.5(C_6H_6)
M	781.8	887.9	887.9	873.9	898.9
Crystal system	Monoclinic	Triclinic	Triclinic	Triclinic	Triclinic
Space group	$P2_1/c$	$P\bar{1}$	$P\bar{1}$	$P\bar{1}$	$P\bar{1}$
a/Å	9.212(5)	10.107(5)	9.596(5)	9.384(5)	9.589(6)
b/Å	15.384(6)	11.121(5)	12.682(6)	12.901(6)	13.179(7)
c/Å	17.735(7)	14.410(7)	13.545(7)	13.415(7)	13.454(7)
α/°	90	74.44(4)	107.47(3)	103.57(2)	110.43(3)
β/°	111.75(2)	72.35(4)	96.61(3)	100.24(3)	100.31(3)
γ/°	90	79.62(3)	106.84(2)	109.04(2)	101.43(3)
V/Å^3	2334(2)	1478(1)	1468(1)	1434(1)	1504(1)
D_c/g cm^{-3}	2.22	1.99	2.01	2.02	1.99
Z	4	2	2	2	2
μ_{Mo}/mm^{-1}	10.233	8.092	8.151	8.340	7.957
$2\theta_{max.}$	48	50	46	50	50
Crystal decay	none	none	none	none	5%
Min., max. trans. factor	0.18, 0.37	0.19, 0.60	0.20, 0.46	0.15, 0.43	0.26, 0.39
Unique refl.	3656	5182	4076	5021	5273
Observed reflections	1727	2676	2481	2545	3538
R_{merge}	0.023	0.025	0.025	0.065	0.022
R	0.062	0.075	0.060	0.079	0.043
R_w	0.068	0.092	0.072	0.095	0.051
CCDC supp. publication no.	201128	201126	201127	201129	201125

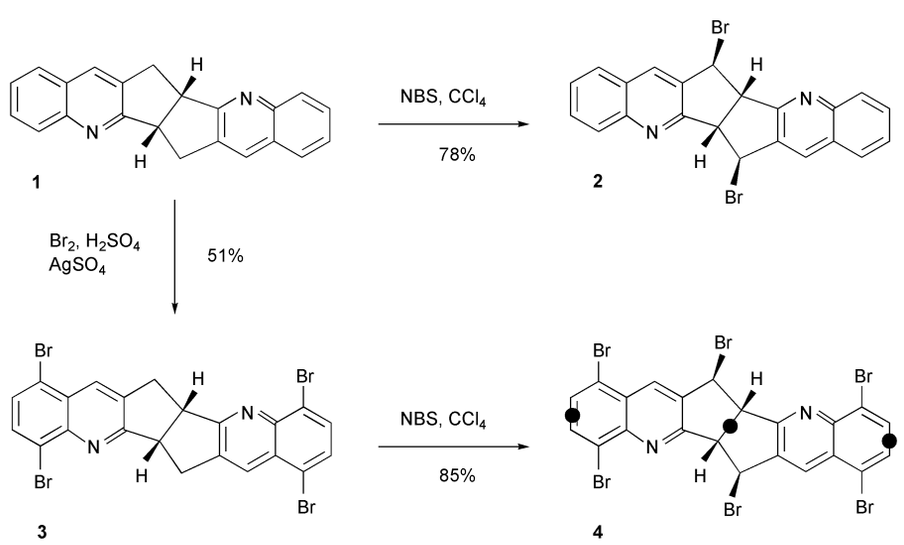

Scheme 1 Preparations of the three diquinoline host molecules **2**–**4**. The black circles added to molecular structure **4** designate the bond centroids used for measuring the fold-angles present in the various crystal structures.

Solutions of several larger aromatics were also tested with **4** (ferrocene in chloroform, hydroquinone in ethyl acetate, anthracene in chloroform, triphenylphosphine in chloroform, and 4,4′-diphenylstilbene in benzene), but no inclusion compounds of these solids were obtained.

Crystal structure of solvent-free 4

Recently, we reported that crystallisation from certain dual-nature solvents can increase the probability of obtaining a lattice inclusion host in its crystalline solvent-free form.[16] This was achieved here when **4** was crystallised from trifluoromethylbenzene, yielding crystals of pure **4** in space group $P2_1/c$.

Molecules of **4** form parallel layers in the *bc* plane, shown edge-on in Fig. 1. Both surfaces of each layer are dense in bromine atoms which form effective multiple Br ··· Br inter-layer contacts (3.52, 3.66, 3.82, 4.03 Å).[21] Part of one layer is projected near the *bc* plane in Fig. 2. This shows that, within the layer, the molecules of **4** are arranged as parallel chains along *b*.

The interactions within each chain are clearly identifiable. In addition to both *exo*,*exo* (3.6 Å) and *endo*,*endo* (3.7 Å) centrosymmetric aromatic offset face–face (OFF) motifs, there are also aromatic edge–face (EF) interactions present (C ··· C 3.7 Å). The two inter-facial contacts are both genuine OFF interactions, as opposed to the related pi–halogen dimer (PHD)[10] motif (encountered later), since the bromine atoms are directed outwards toward the layer surface rather than being oriented towards its centre. In addition, Br ··· Br interactions operate within the chains (4.10 Å *exo*,*exo*-facial; 4.16 Å *endo*,*endo*-facial).

There are fewer identifiable supramolecular synthons where the chains abut. No aryl OFF, EF, or PHD motifs operate, but there are inter-chain Br ··· Br interactions (3.72, 4.03, 4.07 Å), in addition to organic dispersion forces.

Crystal structure of the *o*-xylene compound

Crystallisation of **4** from *o*-xylene gave the 1 : 1 inclusion compound in space group $P\bar{1}$. This structure also contains layers of **4** with Br ··· Br interactions (3.53, 3.55, 3.69, 3.81, 3.84, 3.87 Å) between them (Fig. 3), but the inter-layer halogen network is now less dense due to insertion of the hydrocarbon *o*-xylene guests within the layers.

Once again, the molecules of **4** within each layer are arranged as parallel chains with effective *exo*,*exo*-OFF (3.6 Å),

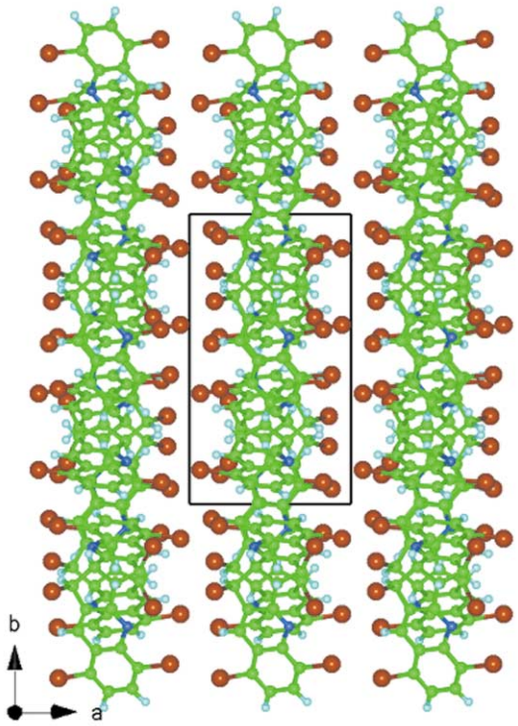

Fig. 1 Projection of the structure of **4** showing the parallel layers edge-on in the *bc* plane. Note the bromine-rich inter-layer regions. Colour code: C green, H pale blue, N dark blue, and Br brown.

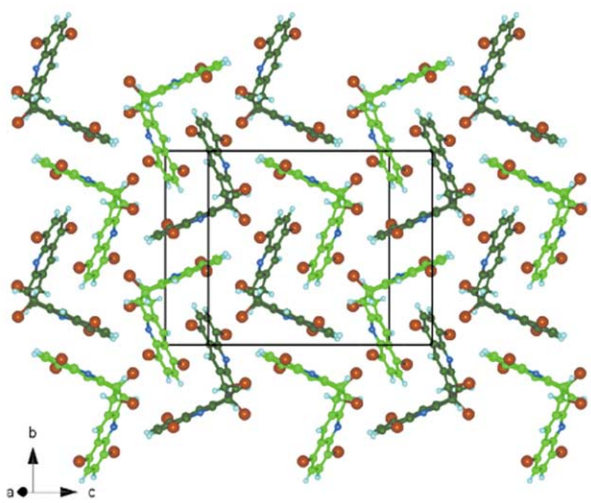

Fig. 2 View of one layer of the structure of **4** (close to the *bc* plane) revealing the parallel chains of **4** molecules along *b*. These are linked by means of OFF and EF interactions, and the carbon atoms of opposite enantiomers are coloured light and dark green.

endo,*endo*-OFF (3.4 Å), and EF (C ··· C 3.8 Å) interactions. In addition, aryl Br ··· Br interactions operate within the chains (3.93 Å *endo,endo*-facial; 4.03 Å *exo,exo*-facial).

The *o*-xylene guest molecules in this crystal structure are disordered over two coplanar positions. They are present as centrosymmetric head–head pairs along the chain direction and lie between the host chains. Insertion of these guest molecules provides host–guest OFF and EF interactions as shown in Fig. 4. Centrosymmetric double Br ··· Br interactions of 4.13 Å also operate between the aliphatic *exo*-bromines of adjacent host chains.

Crystal structure of the toluene and *p*-xylene compounds

Crystallisation of **4** from toluene or from *p*-xylene gave isostructural 1 : 1 inclusion compounds in space group $P\bar{1}$. These structures are generally similar to the *o*-xylene case as can be

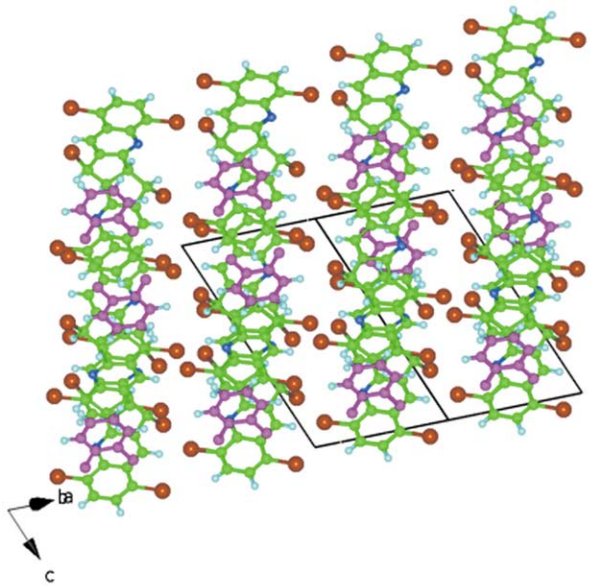

Fig. 3 Projection view showing the molecular layers present in the (**4**)·(*o*-xylene) structure. Here (and in Fig. 4) only one disorder component of the guest is illustrated. Guest carbon atoms are coloured purple. Note the reduced density of the inter-layer Br ··· Br interactions.

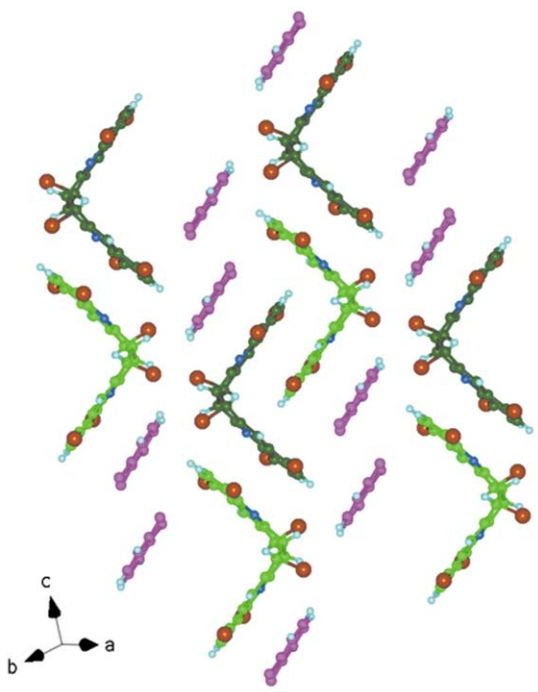

Fig. 4 View of part of one layer in compound (**4**)·(*o*-xylene) with the carbon atoms of opposite enantiomers of **4** coloured light and dark green and the guest carbon atoms coloured purple. The parallel chains of **4** molecules are linked by means of OFF and EF interactions. Addition of the guest molecules now provides host–guest OFF and EF stabilisation between the chains.

seen from the close resemblance of the projections in Figs. 3 and 5.[22]

In (**4**)·(toluene), the interlayer Br ··· Br interactions (see Fig. 5) are 3.59, 3.66, 3.77, 3.84 and 4.03 Å. As before, the molecules of **4** are arranged as parallel chains (see Fig. 6) with intra-chain *exo*,*exo*-OFF (3.7 Å), *endo*,*endo*-OFF (3.5 Å), EF (C ··· C 3.6 Å) and Br ··· Br interactions (4.05 Å *endo,endo*-facial; 4.12 Å *exo,exo*-facial). The host molecules in the chains overlap slightly better here than for the *o*-xylene case. Hence, the first interaction still involves two aryl bromine atoms, but the latter now involves one aryl bromine and one aliphatic

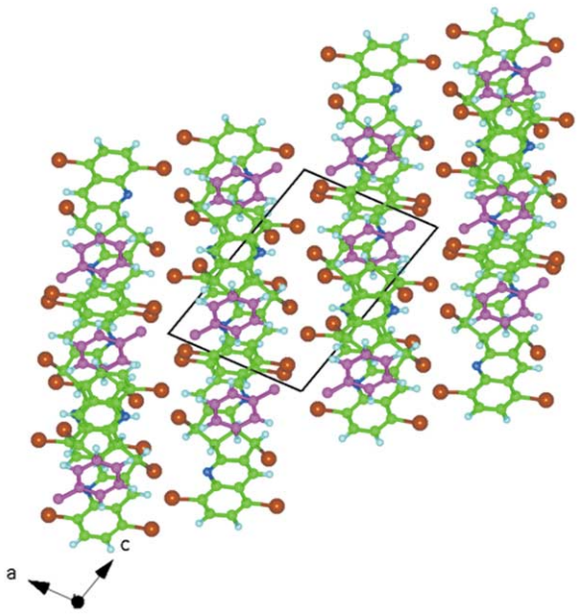

Fig. 5 Edge-on view of the layers present in the structure of (**4**)·(toluene). The carbon atoms of the toluene guest are shown in purple, and its methyl hydrogens are omitted. Comparison with Fig. 1 illustrates the marked reduction in inter-layer bromine atom density as a result of guest inclusion.

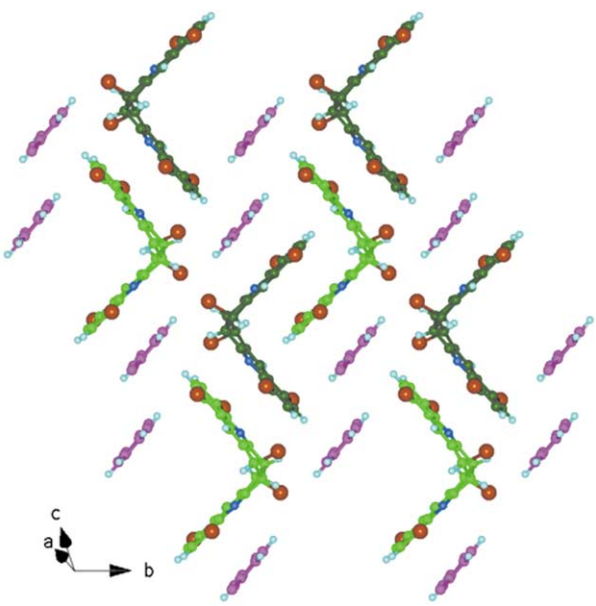

Fig. 6 Part of one layer present in (**4**)·(toluene) showing insertion of the guest molecules between the chains of host molecules, the opposite enantiomers of which are coloured light and dark green. Efficient host–guest OFF and EF interactions link adjacent host chains.

exo-bromine. (Concomitantly, the aryl Br ··· Br *exo*,*exo*-facial distance increases to 4.30 Å, and the inter-chain aliphatic *exo*-bromine Br ··· Br separation to 4.84 Å, so these contribute little to structural stabilisation).

Once again, guest molecules separate the host chains and are present as centrosymmetric pairs along the chain direction. In the case of (**4**)·(toluene), insertion of the guest molecules provides host–guest OFF (3.5 Å) and EF (3.8 and 4.0 C ··· C Å) interactions.

In all three of these inclusion structures, the presence of the aromatic guest molecules produces a common motif that cross-links the layer structure. This is a centrosymmetric unit HOST-EF-GUEST-OFF-HOST-OFF-HOST-OFF-GUEST-EF-HOST that is clearly visible in Figs. 4 and 6 running orthogonal to the host chain direction.

Crystal structure of the benzene compound

Crystallisation of **4** from benzene gave the compound $(\mathbf{4})_2$·(benzene)$_3$ in space group $P\bar{1}$. Concomitant with the increased amount of the smaller guest, there now are two crystallographically independent benzene guest molecules in this structure. Benzene molecules of one type (purple in Fig. 7) lie within the layers as before, while the new type (yellow) lies between the layers for the first time. The latter guests further reduce the density of Br ··· Br interactions, but compensate by providing additional aryl host–guest stabilisation. The inter-layer Br ··· Br interactions have values of 3.55, 3.72 and 3.73 Å.

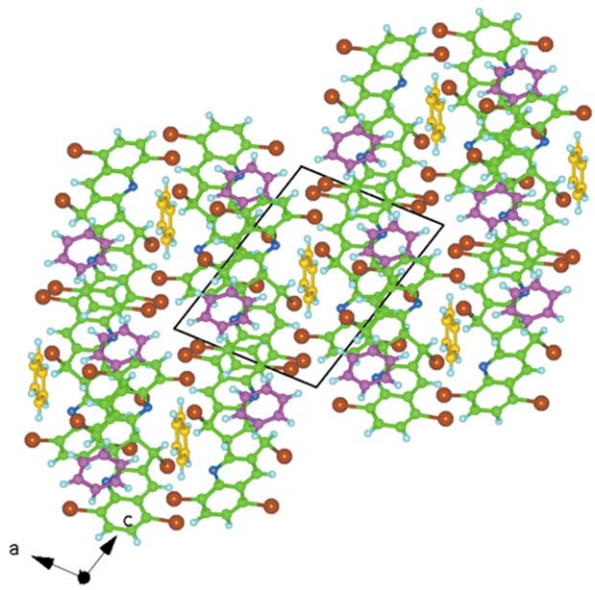

Fig. 7 The layers present in the structure of $(\mathbf{4})_2$·(benzene)$_3$ viewed edge-on. Two crystallographically independent benzene guests are present in this solid. The purple ones within the layers function in the same manner as before, while the yellow ones separate adjacent layers from each other.

Fig. 8 shows the host–guest arrangement within part of one layer. There is a fundamental change to the previous crystal structures in that the host *endo*,*endo*-facial arrangement has

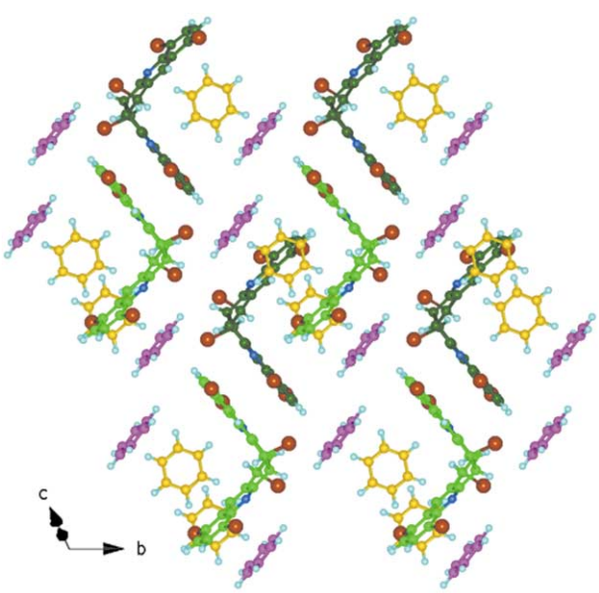

Fig. 8 View of part of one layer in $(\mathbf{4})_2$·(benzene)$_3$ showing the relative orientations of the purple and yellow benzene guest molecules. Both crystallographic types provide significant aryl–aryl host–guest stabilisation in this inclusion compound, leading to the lowest energy structure of the series.

Table 2 Energy (kcal mol^{-1}) and molecular packing calculations for the hexabromo compound **4** and its inclusion compounds

Properties/compound	**4**	(**4**)·(C_8H_{10}) (*o*-xylene)	(**4**)·(C_8H_{10}) (*p*-xylene)	(**4**)·(C_7H_8)	(**4**)$_2$·(C_6H_6)$_3$
Packing coefficient	68%	68%	69%	68%	67%
Van der Waals energy	−186	−119	−122	−121	−131
Coulombic energy (QEq)	−8	−75	−73	−74	−121
Total energy[a]	−194	−195	−195	−195	−252
Unit cell volume /Å^3	2334	1478	1468	1434	1504
Relative packing energy[b]	−83	−132	−133	−136	−168

[a] Calculated crystal packing energy (kcal mol^{-1} of unit cells) .[b] Total energy ÷ unit cell volume/1000. (Packing energy per 1000 Å^3 of the crystal).

switched from an OFF to a PHD (pi–halogen dimer) interaction.[10] In this efficient packing motif, two inversion related host molecules pack so that a bromine atom from each lies within the cleft of its V-shaped partner. Essentially, one OFF and two EF interactions of the host dimer are replaced by four bromine–aryl ring interactions[13] in the new host dimer arrangement. Hence the orthogonal cross-linking motif becomes a centrosymmetric HOST-EF-GUEST-OFF-HOST-PHD-HOST-OFF-GUEST-EF-HOST unit.

Within the host chains there are three *exo*,*exo*-facial interactions (OFF 3.7 Å, aryl Br–aryl Br 4.13 Å, and aryl Br–aliphatic Br 4.12 Å), plus two *endo*,*endo*-facial bromine-ring centroid PHD interactions of 3.48 and 3.60 Å. The host–intralayer guest (purple benzene) interactions are OFF 3.6 and EF 3.9, and the host–interlayer guest (yellow benzene) interaction is EF 3.8 Å, all these values being C ··· C distances.

The *endo*,*endo*-facial arrangements in (**4**)·(toluene) and (**4**)$_2$·(benzene)$_3$ are compared in Fig. 9. Their difference is seen most clearly in the right-hand π-stacking views. The toluene compound (top) has good π-overlap and the central bromine atoms nearly eclipsed, whereas the benzene compound (centre) has poorer π-stacking and staggered central bromine atoms. This is achieved by simple mutual rotation of the two host molecules. A major consequence of PHD generation is concomitant formation of cavities sufficiently large to accommodate the (yellow) inter-layer benzene molecules on both faces of the dimeric motif (see Fig. 9, bottom).

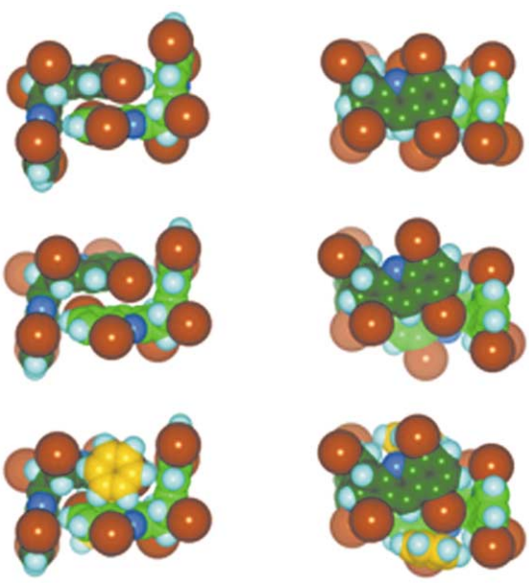

Fig. 9 Comparison of the *endo,endo*-facial interactions in (**4**)·(toluene) (top pair of diagrams) where the aryl–aryl interactions are OFF and EF; and (**4**)$_2$·(benzene)$_3$ (centre diagrams) where the aryl interaction is PHD, thereby forming a cavity in which the interlayer benzene molecule (yellow) is located (bottom diagrams).

Comparison of the crystal structures

Molecule **4** has a slightly twisted V-shaped structure with the potential for conformational adaption to different circumstances. One means of comparison is the fold-angle value present in the various compounds. This is defined as the angle present between the three bond centroids marked on the molecular structure of **4** in Scheme 1. The values of the fold-angles, in the order the compounds are discussed in this paper, are 92.9, 100.3, 102.4, 99.5 and 101.7° respectively. These are comparable to the consistent values observed for the inclusion compounds of diquinoline **2**, despite very different values being potentially accessible to the diquinoline framework.[15] The fold angle for solvent-free **4** (92.9°) is, however, lower than all the inclusion compound cases.

The calculated densities of the four aromatic hydrocarbon inclusion compounds are consistent over the range 1.99 to 2.02 g cm^{-3}. These values are significantly less than pure **4** (2.22 g cm^{-3}) since a less dense guest component has been added. Packing coefficients are also consistent (67–69%) across the series of five compounds. The benzene compound is marginally the worst (67%), but it is the lattice energy that is the ultimate arbiter of the best arrangement.[23]

Crystal lattice energy calculations were performed on the five crystal structures using the Cerius^2 ® package[24] which gave the lattice packing energy per mole of unit cells (Table 2). Since the bigger the volume considered, the larger the energy value obtained, correction to a common standard volume is necessary for a meaningful comparison. Here, the total energy was divided by the unit cell volume/1000, which is equivalent to normalising all five structures at a common volume of 1000 Å^3.

The order of discussion of the compounds in this paper has followed the order of these relative packing energies. Pure **4** has the highest energy (−83 kcal mol^{-1}); the *o*-xylene, *p*-xylene, and toluene compounds have significantly lower, but comparable, energies (−132, −133, −136 kcal mol^{-1}); while the benzene compound has the lowest energy (−168 kcal mol^{-1}) of the series.

Conclusions

These results confirm our view that increasing the number of bromine atoms on the diquinoline skeleton beyond four has an adverse effect on molecular inclusion behaviour. The dibromide **2**[15] and tetrabromide **3**[10,16] include many more guests than the hexabromide **4**. Nonetheless, compound **4** shows a strong preference for inclusion of small aromatic hydrocarbon guests. The reason for this becomes apparent when the crystal structure of the pure substance is compared with those of its inclusion compounds. Although solvent-free **4** forms a good crystal structure it has two structural weaknesses: poor association between the different host chains within its layers, and a high density of Br ··· Br interactions between its layers.

If small aromatic hydrocarbon guests are included within the layers, then there is partial replacement of Br ··· Br contacts by aromatic OFF and EF interactions. The better directional properties of the latter motifs are probably significant in causing energy lowering of the resulting inclusion compounds. The best arrangement found is that present in (**4**)$_2$·(benzene)$_3$ where a greater proportion of the smaller guest can be included. A switch from the classical[8] OFF and EF host–host interaction to the recently described[10] PHD motif now provides sufficient

space for inclusion of additional aromatic guest molecules between the layers.

Experimental section

^{1}H (300 MHz) and ^{13}C (75 MHz) NMR spectra were recorded using a Bruker ACF300 instrument at 25 °C and are reported as chemical shifts (δ) relative to TMS. The substitution of carbon atoms was determined by the DEPT procedure. Melting points were determined with a Kofler instrument and are uncorrected. IR spectra were recorded on a Perkin Elmer 298 infrared spectrophotometer. Low resolution mass spectra (EI) were recorded on a VG Quattro triple quadrupole instrument by Dr J. J. Brophy at UNSW. HRMS measurements were carried out at The Australian National University, Canberra.

1,4,6α,8,11,13α-Hexabromo-5bα,6,12bα,13-tetrahydropentaleno[1,2-*b*:4,5-*b*′]diquinoline (4)

A solution of tetrabromide[10] **3** (0.50 g, 0.80 mmol) and *N*-bromosuccinimide (NBS) (1.00 g, 5.62 mmol) in carbon tetrachloride (150 mL) was refluxed overnight. The reaction mixture was cooled, filtered and the succinimide residue washed with additional CCl_4. Solvent was evaporated from the combined filtrate and washings to yield the crude product which was eluted through a silica gel column using dichloromethane to yield **4** (0.53 g, 85%). Mp 135–136 °C (decomp.). ^{1}H NMR ($CDCl_3$): δ = 4.91 (s, 2H), 6.31 (s, 2H), 7.60 (d, ^3J = 8.3 Hz, 2H), 7.87 (d, ^3J = 8.3 Hz, 2H), 8.50 (s, 2H). ^{13}C NMR ($CDCl_3$): δ = 47.9 (CH), 57.6 (CH), 121.9 (C), 124.6 (C), 128.6 (C), 130.8 (CH), 133.8 (CH), 133.9 (CH), 137.1 (C), 146.7 (C), 163.9 (C). IR (paraffin mull): ν_{max} = 1600w, 1575w, 1290m, 1250m, 1180m, 1135w, 1090s, 990w, 905s, 875m, 820s, 780m, 745s, 705w cm^{-1}. MS: *m*/*z* (>320 and >20%) = 784 (M^+, two ^{79}Br/four ^{81}Br, 21%), 782 (M^+, three ^{79}Br/three ^{81}Br, 35), 780 (M^+, four ^{79}Br/two ^{81}Br, 30), 705 (49), 704 (30), 703 (100), 702 (36), 701 (88), 699 (37), 624 (43), 623 (46), 622 (56), 621 (55), 620 (46), 619 (27), 543 (21), 541 (21), 464 (29), 463 (46), 462 (64), 461 (57), 460 (28), 459 (26), 383 (45), 382 (51), 381 (56), 380 (38). $C_{22}H_{10}N_2Br_6$ (FW 781.8) HRMS: *m*/*z* calc. for M^+ $(C_{22}H_{10}N_2Br_6)^+$ 785.584185 (one ^{79}Br/five ^{81}Br), 783.586231 (two ^{79}Br/four ^{81}Br), 781.588277 (three ^{79}Br/three ^{81}Br), 779.590323 (four ^{79}Br/two ^{81}Br), 777.592369 (five ^{79}Br/one ^{81}Br); found: 785.584761, 783.586510, 781.588588, 779.590458, 777.592099. Crystals of the individual inclusion compounds for X-ray study were grown by slow evaporation of solutions of **4** in the relevant solvent.

Structure determinations

For all structures, reflection data were measured with an Enraf-Nonius CAD-4 diffractometer in $\theta/2\theta$ scan mode using graphite monochromated molybdenum radiation (λ = 0.7107 Å). Data were corrected for absorption.[25] Reflections with $I > 2\sigma(I)$ were considered observed. The structures were determined by direct phasing (SIR92)[26] and Fourier methods. Hydrogen atoms for each structure were included in calculated positions. Atoms of each host molecule were refined with independent positional parameters; individual anisotropic temperature parameters were assigned to the bromine atoms, and a 15-parameter *TLX* rigid-body thermal parameter (where *T* is the translation tensor, *L* is the libration tensor and *X* is the origin of libration) described the thermal motion of the remaining atoms.[27] The guest molecules were modelled as planar rigid groups with the thermal motion of each defined by a *TLX* rigid group. For (**4**)·(*o*-xylene) the guest was disordered in two overlapping sites with equal occupancy. Reflection weights used were $1/\sigma^2(F_o)$, with $\sigma(F_o)$ being derived from $\sigma(I_o) = [\sigma^2(I_o) + (0.04I_o)^2]^{1/2}$. The weighted residual was defined as $R_w = (\Sigma w\Delta^2/\Sigma wF_o^2)^{1/2}$. Atomic scattering factors and anomalous dispersion parameters were from International Tables for X-ray Crystallography.[28] CCDC-201125–201129 (see compound listing in Table 1) contain the supplementary crystallographic data for this paper. †

Energy calculations

Intermolecular potential for atoms *i*, *j* with charges q_i, q_j separated by d_{ij} is given by equation (1), and comprises the van der Waals and coulombic energies. The atom parameters e^a (kcal mol^{-1}), r^a (Å), are: C, 0.095, 1.95; N, 0.077, 1.83; H, 0.015, 1.60; Br, 0.370, 1.98. The combination rules are given in equations (2) and (3). The permittivity ε in eqn. (1) = 1.

$$E_{ij} = e^a_{ij}\,[(d_{ij}/d^a_{ij})^{-12} - 2(d_{ij}/d^a_{ij})^{-6}] + (q_i \cdot q_j)/(\varepsilon \cdot d_{ij}) \quad (1)$$

$$d^a_{ij} = r^a_i + r^a_j \quad (2)$$

$$e^a_{ij} = (e^a_i \cdot e^a_j)^{0.5} \quad (3)$$

Atom partial charges *q* were calculated using the QEq procedure of Rappe and Goddard,[29] as implemented in the MSI Cerius^2 ® software.[24] This method of equalisation of chemical potential is responsive to geometry. The lattice energy computed was normalised to allow for variation in cell volume: the values quoted are energy per 1000 Å^3. Since the crystal densities are similar, this compensates for the fact that the energy calculations for the different structures incorporated different numbers of atoms.

† CCDC reference numbers 201125–201129. See http://www.rsc.org/suppdata/ob/b3/b300248a/ for crystallographic data in .cif or other electronic format.

Acknowledgements

We gratefully acknowledge financial support from the Australian Research Council.

References and notes

1 *Inclusion Compounds*, eds. J. L. Atwood, J. E. D. Davies and D. D. MacNicol, vol. 1–3, Academic Press, London, 1984; *Inclusion Compounds*, eds. J. L. Atwood, J. E. D. Davies and D. D. MacNicol, Vol. 4–5, Oxford University Press, Oxford, 1991.
2 *Comprehensive Supramolecular Chemistry*, vol. 6 : *Solid State Supramolecular Chemistry: Crystal Engineering*, eds. D. D. MacNicol, F. Toda and R. Bishop, Pergamon, Oxford, 1996.
3 I. Goldberg, in *Inclusion Compounds*, eds. J. L. Atwood, J. E. D. Davies and D. D. MacNicol, Oxford University Press, Oxford, 1991, Vol. 4, Ch. 10, pp. 406–447.
4 R. Bishop, *Chem. Soc. Rev.*, 1996, **25**, 311–319.
5 C. E. Marjo, R. Bishop, D. C. Craig and M. L. Scudder, *J. Chem. Soc., Perkin Trans. 2*, 1997, 2099–2104.
6 S. F. Alshahateet, R. Bishop, D. C. Craig and M. L. Scudder, *Cryst. Eng. Comm.*, 2001, **3**(48), 225–229.
7 A. N. M. M. Rahman, R. Bishop, D. C. Craig, C. E. Marjo and M. L. Scudder, *Cryst. Growth Des.*, 2002, **2**, 421–426.
8 G. R. Desiraju and A. Gavezzotti, *Acta Crystallogr., Sect. B*, 1989, **45**, 473–482.
9 C. A. Hunter, K. R. Lawson, J. Perkins and C. J. Urch, *J. Chem. Soc., Perkin Trans. 2*, 2001, 651–669.
10 A. N. M. M. Rahman, R. Bishop, D. C. Craig and M. L. Scudder, *Cryst. Eng. Comm.*, 2002, **4**(84), 510–513.
11 B. S. Green and G. M. J. Schmidt, *Tetrahedron Lett.*, 1970, 4249–4252.
12 J. A. R. P. Sarma and G. R. Desiraju, *Acc. Chem. Res.*, 1986, **19**, 222–228.
13 R. K. R. Jetti, A. Nangia, F. Xue and T. C. W. Mak, *Chem. Commun.*, 2001, 919–920.
14 A. N. M. M. Rahman, R. Bishop, D. C. Craig and M. L. Scudder, *Chem. Commun.*, 1999, 2389–2390.
15 A. N. M. M. Rahman, R. Bishop, D. C. Craig and M. L. Scudder, *Eur. J. Org. Chem.*, 2003, 72–81.
16 R. Bishop, A. N. M. M. Rahman, J. Ashmore, D. C. Craig and M. L. Scudder, *Cryst. Eng. Comm.*, 2002, **4**(101), 605–609.

17 P. B. D. de la Mare, M. Kiamud-din and J. H. Ridd, *Chem. Ind. (London)*, 1958, 361.
18 P. B. D. de la Mare, M. Kiamud-din and J. H. Ridd, *J. Chem. Soc.*, 1960, 561–565.
19 C. E. Marjo, A. N. M. M. Rahman, R. Bishop, M. L. Scudder and D. C. Craig, *Tetrahedron*, 2001, **57**, 6289–6293.
20 *Crystal data*. $(\mathbf{4})_2$·(allyl cyanide): $(C_{22}H_{10}Br_6N_2)_2$·(C_4H_5N), M 1630.6, $C2/c$, a 23.053(8) Å, b 17.754(6) Å, c 14.589(5) Å, β 122.66(2)°, V 5027(3) Å^3. Poor crystal quality prevented refinement to acceptable limits. The material is a staircase inclusion compound,[7] rather similar in structure to $(\mathbf{3})_2$·(allyl cyanide)[10] but with small differences in staircase arrangement and guest incorporation.
21 An arbitrary Br ··· Br cut-off value of 4.20 Å is used throughout this paper.
22 Comparable Figures for (**4**)·(*p*-xylene) may be generated from the deposited crystal data. Compound (**4**)·(*o*-xylene) can be considered as a crystallographic permutation of (**4**)·(toluene) or (**4**)·(*p*-xylene). The transformation $\boldsymbol{a}_n = \boldsymbol{c}$, $\boldsymbol{b}_n = -\boldsymbol{a} + \boldsymbol{b}$, $\boldsymbol{c}_n = \boldsymbol{a} + \boldsymbol{b}$ leads to a (non-reduced) cell with a_n = 14.4, b_n = 13.6, c_n = 16.3 Å, α_n = 96, β_n = 112, γ_n = 90° which can be compared directly with the cells of the other two compounds.
23 J. D. Dunitz, G. Filippini and A. Gavezzotti, *Tetrahedron*, 2000, **56**, 6595–6601.
24 Cerius^2 ® version 3.8, http://www.accelrys.com.
25 J. De Meulenaer and M. Tompa, *Acta Crystallogr.*, 1965, **19**, 1014–1018.
26 A. Altomare, G. Cascarano, C. Giacovazzo, A. Guagliardi, M. C. Burla, G. Polidori and M. Camalli, *J. Appl. Cryst.*, 1994, **27**, 435.
27 A. D. Rae, *RAELS. A Comprehensive Constrained Least Squares Refinement Program*, Australian National University, Canberra, Australia, 2000.
28 *International Tables for X-Ray Crystallography*, Vol. 4, eds. J. A. Ibers, W. C. Hamilton, Kynoch Press, Birmingham, 1974.
29 A. K. Rappe and W. A. Goddard, *J. Phys. Chem.*, 1991, **95**, 3358–3363.